Randomized iterative feedback tuning for fast MIMO feedback design of a mechatronic system

Aarnoudse, Leontine; den Toom, Peter; Oomen, Tom

DOI
10.1016/j.conengprac.2024.106152

Publication date
2025

Document Version
Final published version

Published in
Control Engineering Practice

Control Engineering Practice 154 (2025) 106152

Contents lists available at ScienceDirect

Control Engineering Practice

journal homepage: www.elsevier.com/locate/conengprac

Randomized iterative feedback tuning for fast MIMO feedback design of a mechatronic system ☆

Leontine Aarnoudse [a,*], Peter den Toom [a], Tom Oomen [a,b]

[a] Department of Mechanical Engineering, Control Systems Technology, Eindhoven University of Technology, Eindhoven, The Netherlands
[b] Delft Center for Systems and Control, Delft University of Technology, Delft, The Netherlands

ARTICLE INFO

Keywords:
Iterative feedback tuning
MIMO systems
Gradient estimation
Data-driven control

ABSTRACT

Iterative feedback tuning (IFT) enables the tuning of feedback controllers using only measured data to obtain the gradient of a cost criterion. The aim of this paper is to reduce the required number of experiments for MIMO IFT. It is shown that, through a randomization technique, an unbiased gradient estimate can be obtained from a single dedicated experiment, regardless of the size of the MIMO system. The gradient estimate is used in a stochastic gradient descent algorithm. The approach is experimentally validated on a mechatronic system, showing a significantly reduced number of experiments compared to standard IFT.

1. Introduction

Data-driven methods for feedback controller design are appealing because their limited dependency on accurate modeling. In contrast to data-driven methods, fully model-based feedback design requires accurate models that are typically obtained through system identification, an expensive and difficult process, especially for multiple-input multiple-output (MIMO) systems. Data-driven approaches often use approximate models in conjunction with measured data, leading to less stringent modeling requirements. Some data-driven control methods include frequency-domain tuning (Kammer, Bitmead, & Bartlett, 1998), virtual-reference feedback tuning (VRFT) (Campi, Lecchini, & Savaresi, 2002; Formentin & Savaresi, 2011), correlation-based tuning (Mišković, Karimi, Bonvin, & Gevers, 2007) and iterative feedback tuning (IFT) (Hjalmarsson & Birkeland, 1998; Hjalmarsson & Kan Hjalmarsson, 1999), see also Sanfelice Bazanella, Campestrini, and Eckhard (2012) for an overview. This paper focuses on IFT, an optimization-based approach that tunes the feedback controller parameters to minimize a cost function aimed at tracking or disturbance rejection. In contrast to the other methods, IFT does not require an explicit model, yet it can be interpreted as using local modeling of the dependence of closed-loop signals on the controller (Hjalmarsson, 2005).

The key mechanism of iterative feedback tuning is that the gradient of the cost function can be obtained directly from system experiments. This measured gradient is used in an iterative optimization-based algorithm, typically based on stochastic gradient descent when iteration-varying system disturbances are taken into account. Experimental gradients are available for both single-input single output (SISO) and MIMO systems, yet most applications and extensions are limited to SISO systems. Some examples of successful implementations include applications for the process industry (Hjalmarsson, Gevers, Gunnarsson, & Lequin, 1998) and motion systems (Hamamoto, Fukuda, & Sugie, 2003; Heertjes, Van Der Velden, & Oomen, 2016; Kissling, Blanc, Myszkorowski, & Vaclavik, 2009; Roman et al., 2022), cascaded control for quadrotors (Tesch, Eckhard, & Guarienti, 2016) and robotic systems (Xie, Jin, Tang, Ye, & Tao, 2019), intelligent PID control (Baciu & Lazar, 2023) and even control of nonlinear systems (Codrons, De Bruyne, De Wan, & Gevers, 1998). Extensions of IFT consider, e.g., robustness (Heertjes et al., 2016), system constraints (Xie et al., 2019), convergence speed (Huusom, Hjalmarsson, Poulsen, & Jørgensen, 2011) and, for the specific case of disturbance rejection, methods for optimal prefiltering (Hildebrand, Lecchini, Solari, & Gevers, 2004) and measuring unbiased Hessian estimates (Solari & Gevers, 2004).

IFT is typically only applied to SISO systems, because MIMO IFT is highly inefficient. MIMO IFT requires $n_i \times n_o$ experiments per iteration to measure the gradient for a system with n_i inputs and n_o outputs (Hjalmarsson & Birkeland, 1998), resulting in poor scaling for large MIMO systems since the number of dedicated experiments increases with the size of the system. Related methods that generate gradients for MIMO systems through experiments suffer from the same limitation, examples include VRFT (Formentin, Bisoffi, & Oomen, 2015), H_∞-norm estimation (Oomen, Van Der Maas, Rojas, & Hjalmarsson, 2014) and data-driven iterative learning control (ILC) (Bolder, Kleinendorst, & Oomen, 2018).

☆ This work is part of the research programme VIDI with project number 15698, which is (partly) financed by the NWO, The Netherlands.
* Corresponding author.
E-mail address: l.i.m.aarnoudse@tue.nl (L. Aarnoudse).

https://doi.org/10.1016/j.conengprac.2024.106152
Received 5 July 2024; Received in revised form 16 September 2024; Accepted 23 October 2024
Available online 6 November 2024

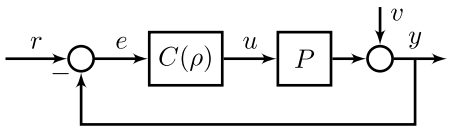

Fig. 1. Control scheme.

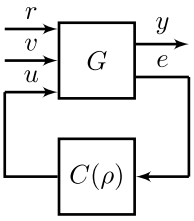

Fig. 2. General control scheme.

Randomization based on insights from simultaneous perturbation stochastic approximation (SPSA) (Spall, 1988) can reduce the required number of experiments to obtain experimental gradients for MIMO systems significantly. In SPSA, an unbiased gradient estimate is obtained by perturbing all parameters simultaneously in random directions. An SPSA-based randomized MIMO IFT algorithm that aims at reducing the number of dedicated experiments is introduced in Gerencsér, Vágó, and Hjalmarsson (2002). However, this approach is limited to systems with periodic reference signals and negligible measurement noise, and it is unclear how the unbiased gradient estimates are obtained. In the current paper, it is shown that an unbiased gradient estimate for MIMO IFT can be obtained from a single experiment, regardless of the size of the system. A similar idea is developed for data-driven MIMO iterative learning control (ILC) in Aarnoudse and Oomen (2021). The unbiased gradient estimates are used in a stochastic gradient descent algorithm (Robbins & Monro, 1951), for which convergence can be shown. The method is reminiscent of SPSA, but it is fundamentally different because it retains the gradient expressions from MIMO IFT and does not replace them with less accurate parameter perturbations.

Although significant steps have been taken towards fully data-driven tuning of feedback controllers for MIMO systems, an efficient method without scaling issues for large MIMO systems is lacking. The aim of this paper is to develop an efficient MIMO iterative feedback tuning method that requires only a single experiment per iteration to obtain an unbiased gradient estimate. The contribution consists of the following elements.

- A new approach is developed for fast MIMO IFT that requires a single experiment per iteration to obtain an unbiased gradient estimate.
- A convergence proof of the presented algorithm is obtained.
- Experimental validation and comparison to standard MIMO IFT of the presented approach.

Preliminary results are presented in Aarnoudse and Oomen (2023), which introduces a single experiment to obtain an unbiased gradient estimate for MIMO IFT. The present paper extends these results by experimental implementation on a mechatronic system, detailed explanations in the form of illustrations and procedures for the presented method, an adapted method that reduces the variance when not all MIMO controller channels are used, and consideration of the problem of robust optimization.

The paper is structured as follows. In Section 2, the considered problem is introduced. In Section 3, a new method to efficiently obtain gradient estimates for MIMO IFT is presented. Section 4 applies these gradient estimates in a stochastic approximation IFT algorithm. The presented method is compared to standard MIMO IFT in Section 5, in which also the case of non-full controllers is considered. In Section 6, implementation aspects are discussed. Experimental results are presented in Section 7 and finally, conclusions are given in Section 8.

2. Problem formulation

The problem considered in this paper is the data-based optimization of the parameters of a feedback controller $C(\rho)$ for an unknown discrete-time linear time-invariant MIMO system $P(q)$, given by

$$\underbrace{\begin{bmatrix} y_1(t) \\ y_2(t) \\ \vdots \\ y_{n_o}(t) \end{bmatrix}}_{y(t)} = \underbrace{\begin{bmatrix} P_{11}(q) & \dots & P_{1n_i}(q) \\ \vdots & \ddots & \vdots \\ P_{n_o1}(q) & \dots & P_{n_on_i}(q) \end{bmatrix}}_{P(q)} \underbrace{\begin{bmatrix} u_1(t) \\ u_2(t) \\ \vdots \\ u_{n_i}(t) \end{bmatrix}}_{u(t)} + \underbrace{\begin{bmatrix} v_1(t) \\ v_2(t) \\ \vdots \\ v_{n_o}(t) \end{bmatrix}}_{v(t)}, \tag{1}$$

with q denoting the shift operator, input $u(t) \in \mathbb{R}^{n_i}$, output $y(t) \in \mathbb{R}^{n_o}$ and disturbance $v(t) \in \mathbb{R}^{n_o}$, as illustrated in Fig. 1. System P has n_i inputs and n_o outputs, and the controller $C(\rho)$ is parameterized by a parameter vector $\rho \in \mathbb{R}^{n_\rho}$. The aim is to find the controller parameters ρ that minimize the cost function

$$\mathcal{J}(\rho) = \frac{1}{2N} \sum_{t=1}^{N} \left[(r(t) - y(\rho, t))^{\mathsf{T}} (r(t) - y(\rho, t)) \right], \tag{2}$$

with reference $r(t) \in \mathbb{R}^{n_o}$. When $C(q, \rho)$ is connected to $P(q)$ using negative feedback, the output $y(t)$ can be rewritten as

$$\begin{aligned} y(t) =& (I + P(q)C(q, \rho))^{-1} P(q)C(q, \rho)r(t) + \\ & (I + P(q)C(q, \rho))^{-1} v(t), \end{aligned} \tag{3}$$

The feedback error $e(t) \in \mathbb{R}^{n_o}$ is given by $e(t) = r(t) - y(t)$. In the remainder of this paper, the time t and shift operator q are omitted when not needed for brevity of notation.

The aim of this paper is to develop an experimentally inexpensive approach to minimizing (2) for an unknown MIMO system, i.e., it is assumed that no model of P is available. A gradient-based approach based on iterative feedback tuning (IFT) is used, in which the experimentally expensive gradient expressions are replaced by gradient estimates that follow from a single experiment.

Remark 1. Many SISO IFT applications use a two-degree-of-freedom (DOF) controller structure, for which a reference model is necessary. The focus of this paper is on MIMO mechatronic systems with single-DOF controllers, therefore reference models are omitted. All results can be extended to the case with reference models, for which $r(t)$ in the cost function (2) is replaced by $y_d(t) = M(q)r(t)$ for reference model $M(q)$ and desired output $y_d(t)$.

3. Efficient gradient estimates for MIMO iterative feedback tuning

In this section, an efficient method to minimizing (2) for unknown MIMO systems is introduced. The method is derived from iterative feedback tuning, yet it improves the efficiency significantly through unbiased gradient estimates that follow from a single dedicated experiment. The main result is given in Theorem 1 in Section 3.3, and constitutes the first contribution. To obtain this result, gradient expressions are derived in Section 3.1, and the gradient estimates are illustrated for a 2×2 example in Section 3.2 before extending this to MIMO systems of any size in Section 3.3.

3.1. Gradient expressions for MIMO IFT

The gradient $g(\rho) = \frac{\partial J(\rho)}{\partial \rho}$ of (2) is given by

$$g(\rho) = \frac{1}{N}\sum_{t=1}^{N}\left[-\left(\frac{\partial y(\rho)}{\partial \rho}(t)\right)^{\mathsf{T}}(r(t) - y(\rho, t))\right]. \tag{4}$$

The term $r - y(\rho)$ in (4) is the error signal e from an experiment with reference r and controller $C(\rho)$ and can therefore be measured directly. To illustrate how the term $\frac{\partial y(\rho)}{\partial \rho}(t)$ can be obtained through experiments, the system is rewritten to the generalized plant G with feedback controller $C(\rho)$, shown in Fig. 2, for which

$$\begin{pmatrix} y \\ e \end{pmatrix} = \underbrace{\begin{bmatrix} 0 & I & P \\ I & -I & -P \end{bmatrix}}_{G}\begin{pmatrix} r \\ v \\ u \end{pmatrix}, \tag{5}$$

$$u = C(\rho)e, \tag{6}$$

with $u(t) \in \mathbb{R}^{n_i}$ denoting the controller output. The derivative $\frac{\partial y(\rho)}{\partial \rho}(t) \in \mathbb{R}^{n_o \times N_\rho}$ is of the form

$$\frac{\partial y(\rho)}{\partial \rho}(t) = \begin{bmatrix} y'(\rho(1))(t) & y'(\rho(2))(t) & \dots & y'(\rho(n_\rho))(t) \end{bmatrix}, \tag{7}$$

with $y'(\rho(x))(t) \in \mathbb{R}^{n_o}$ denoting the derivative of $y(\rho)$ to the xth parameter in ρ. For each of these derivatives to a single parameter, it holds that

$$\begin{pmatrix} y' \\ e' \end{pmatrix} = G\begin{pmatrix} 0 \\ 0 \\ u' \end{pmatrix} \tag{8}$$

$$u' = C'(\rho(x))e + C(\rho)e', \tag{9}$$

where the index $\rho(x)$ is omitted for all signals for brevity, and where $C'(\rho(x))$ denotes the derivative of $C(\rho)$ to the xth entry of ρ. From (8), it follows that

$$y'(\rho(x)) = S(\rho)PC'(\rho(x))e, \tag{10}$$

with $S(\rho) = (1 + PC(\rho))^{-1}$. Eq. (10) shows that for each parameter, the derivative can be obtained from an experiment with $r = 0$, where $C'(\rho(x))e$ is injected between the plant and the controller. Rewriting (10) gives

$$y'(\rho(x)) = \begin{pmatrix} \sum_{l=1}^{n_o}\sum_{k=1}^{n_i}(S(\rho)P)_{1k}C'_{kl}(\rho(x))e_l(\rho) \\ \sum_{l=1}^{n_o}\sum_{k=1}^{n_i}(S(\rho)P)_{2k}C'_{kl}(\rho(x))e_l(\rho) \\ \vdots \\ \sum_{l=1}^{n_o}\sum_{k=1}^{n_i}(S(\rho)P)_{n_ok}C'_{kl}(\rho(x))e_l(\rho) \end{pmatrix}, \tag{11}$$

in which the derivatives C'_{kl} are the SISO elements of C', such that C'_{kl} and $(S(\rho)P)_{mk}$ commute. It follows that in order to find the derivative from y to each of the parameters in ρ, and with that the gradient of (2), it is only necessary to obtain the terms $(S(\rho)P)_{mk}e_l(\rho)$ for $m = 1, \dots, n_o$, $k = 1, \dots, n_i$, and $l = 1, \dots, n_o$.

3.2. Efficient unbiased gradient estimates: 2 × 2 example

Next, it is shown how a single experiment leads to unbiased gradient estimates for a 2 × 2 system. The key point is the introduction of a matrix $A \in \mathbb{R}^{2\times 2}$, which for the 2 × 2 system is of the form

$$A = \begin{bmatrix} a^{11} & a^{12} \\ a^{21} & a^{22} \end{bmatrix}. \tag{12}$$

The entries of A are samples from a symmetric Bernoulli ±1 distribution, i.e., $a^{lm} \in \{-1, 1\}$ with probabilities $P(a^{lm} = 1) = 1/2$ and $P(a^{lm} = -1) = 1/2$. Matrix A is time-invariant and iteration-varying, i.e., when the gradient estimates that are developed next are applied in iterative feedback tuning, each iteration j uses a different random matrix A_j.

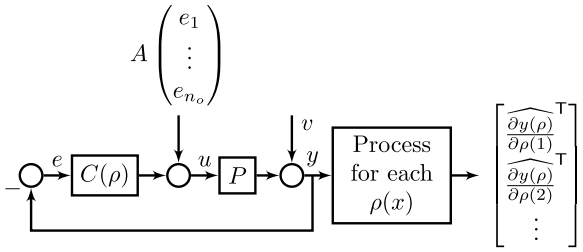

Fig. 3. Stochastic approximation IFT experiment that leads to an unbiased gradient estimate. The experiment corresponds to Eq. (26) and the post-processing is according to (20), respectively (14) and (15) for the 2 × 2 example.

The derivative to a single parameter $y'(\rho(x))(t) \in \mathbb{R}^2$ for a 2 × 2 system is given by

$$y'(\rho(x)) = \begin{bmatrix} (SP)_{11}(C'_{11}e_1 + C'_{12}e_2) + (SP)_{12}(C'_{21}e_1 + C'_{22}e_2) \\ (SP)_{21}(C'_{11}e_1 + C'_{12}e_2) + (SP)_{22}(C'_{21}e_1 + C'_{22}e_2) \end{bmatrix}, \tag{13}$$

where C'_{11} denotes the derivative of the $(1, 1)$ element of C to $\rho(x)$. The dependence on $\rho(x)$ in these derivatives and in S and e is omitted for brevity. The terms $(S(\rho)P)_{mk}(\rho)e_l(\rho)$ for $m = 1, 2$, $k = 1, 2$, and $l = 1, 2$ can be obtained from a single experiment using A as follows:

$$\begin{bmatrix} (SP)_{11} & (SP)_{12} \\ (SP)_{21} & (SP)_{22} \end{bmatrix} A \begin{pmatrix} e_1 \\ e_2 \end{pmatrix} = \begin{bmatrix} (SP)_{11}(a^{11}e_1 + a^{12}e_2) + (SP)_{12}(a^{21}e_1 + a^{22}e_2) \\ (SP)_{21}(a^{11}e_1 + a^{12}e_2) + (SP)_{22}(a^{21}e_1 + a^{22}e_2) \end{bmatrix}. \tag{14}$$

In this experiment, the signal Ae is added to the signal u, i.e., it is injected between the controller and the plant as illustrated in Fig. 3.

The output of this experiment is processed to give an unbiased estimate $\hat{y}'(\rho(x))$ for each parameter $\rho(x)$, $x = 1, 2, \dots, n_\rho$. The estimates are given by

$$\hat{y}'(\rho(x)) = \begin{bmatrix} \left(a_j^{11}C'_{11} + a_j^{12}C'_{12} + a_j^{21}C'_{21} + a_j^{22}C'_{22}\right) \times \\ \left(a_j^{11}C'_{11} + a_j^{12}C'_{12} + a_j^{21}C'_{21} + a_j^{22}C'_{22}\right) \times \\ \left((SP)_{11}(a_j^{11}e_1 + a_j^{12}e_2) + (SP)_{12}(a_j^{21}e_1 + a_j^{22}e_2)\right) \\ \left((SP)_{21}(a_j^{11}e_1 + a_j^{12}e_2) + (SP)_{22}(a_j^{21}e_1 + a_j^{22}e_2)\right) \end{bmatrix}. \tag{15}$$

The expected value of this expression is obtained by noting that $E\{a^{\alpha\beta}a^{\gamma\delta}\} = 1$ if $\alpha = \gamma$, $\beta = \delta$ and otherwise, if $\alpha \neq \gamma$ and/or $\beta \neq \delta$, $E\{a^{\alpha\beta}a^{\gamma\delta}\} = 0$. This gives

$$\begin{aligned} E\{\hat{y}'(\rho(x))\} = & \\ & \begin{bmatrix} a_j^{11}C'_{11}(SP)_{11}a_j^{11}e_1 + a_j^{12}C'_{12}(SP)_{11}a_j^{12}e_2 \\ a_j^{11}C'_{11}(SP)_{21}a_j^{11}e_1 + a_j^{12}C'_{12}(SP)_{21}a_j^{12}e_2 \\ \quad + a_j^{21}C'_{21}J_{12}a_j^{21}e_1 + a_j^{22}C'_{22}(SP)_{12}a_j^{22}e_2 \\ \quad + a_j^{21}C'_{21}J_{22}a_j^{21}e_1 + a_j^{22}C'_{22}(SP)_{22}a_j^{22}e_2 \end{bmatrix} \\ = & \begin{bmatrix} (SP)_{11}(C'_{11}e_1 + C'_{12}e_2) + (SP)_{12}(C'_{21}e_1 + C'_{22}e_2) \\ (SP)_{21}(C'_{11}e_1 + C'_{12}e_2) + (SP)_{22}(C'_{21}e_1 + C'_{22}e_2) \end{bmatrix}, \end{aligned} \tag{16}$$

i.e., $E\{\hat{y}'(\rho(x))\} = y'(\rho(x))$. These estimated derivatives of the output y to each parameter are used to construct an estimate of $\frac{\partial y(\rho)}{\partial \rho}$ of the form

$$\widehat{\frac{\partial y(\rho)}{\partial \rho}}(t) = \begin{bmatrix} \hat{y}'(\rho(1))(t) & \hat{y}'(\rho(2))(t) & \dots & \hat{y}'(\rho(n_\rho))(t) \end{bmatrix}, \tag{17}$$

which is used to construct an unbiased estimate of the gradient $g(\rho)$ in (4) of cost function $\mathcal{J}(\rho)$ in (2), given by

$$\hat{g}(\rho) = \frac{1}{N}\sum_{t=1}^{N}\left[-\left(\widehat{\frac{\partial y(\rho)}{\partial \rho}}(t)\right)^{\mathsf{T}}(r(t) - y(\rho, t))\right]. \tag{18}$$

Since $E\{\hat{y}'(\rho(x))\} = y'(\rho(x))$, $\hat{g}(\rho)$ is an unbiased estimator of $\hat{g}(\rho)$. Thus, a single experiment (14) leads to an unbiased estimate of the gradient (4), which can be used to minimize the cost function (2) through stochastic approximation as shown in Section 4. Next, the approach is extended to general MIMO systems.

3.3. Efficient unbiased gradient estimates for MIMO IFT

The approach that is illustrated for a 2×2 system can be extended to general $n_i \times n_o$ MIMO systems directly. The general form of the matrix $A \in \mathbb{R}^{(n_i)\times(n_o)}$ is as follows.

$$A = \begin{bmatrix} a^{11} & \dots & a^{1n_o} \\ \vdots & \ddots & \vdots \\ a^{n_i 1} & \dots & a^{n_i n_o} \end{bmatrix}. \tag{19}$$

Again, the entries a^{lm} are samples from a symmetric Bernoulli ± 1 distribution, such that $a^{lm} \in \{-1, 1\}$ with probabilities $P(a^{lm} = 1) = 1/2$ and $P(a^{lm} = -1) = 1/2$, and matrix A is time-invariant and iteration-varying. The following theorem formalizes the results for general MIMO systems.

Theorem 1. *Let*

$$\hat{y}'(\rho(x)) = \begin{bmatrix} \sum_{m=1}^{n_i}\sum_{q=1}^{n_o} a^{mq} C'_{mq}\left(\sum_{k=1}^{n_i}(SP)_{1k}\left(\sum_{l=1}^{n_o} a^{kl} e_l\right)\right) \\ \vdots \\ \sum_{m=1}^{n_i}\sum_{q=1}^{n_o} a_j^{mq} C'_{mq}\left(\sum_{k=1}^{n_i}(SP)_{n_o k}\left(\sum_{l=1}^{n_o} a^{kl} e_l\right)\right) \end{bmatrix}, \tag{20}$$

with a^{mq} and a^{kl} the entries of matrix A in (19), and define

$$\hat{g}(\rho) = \frac{1}{N}\sum_{t=1}^{N}\left[\left(\widehat{\frac{\partial y(\rho)}{\partial \rho}}(t)\right)^{\mathsf{T}}(r(t) - y(\rho, t))\right], \tag{21}$$

with

$$\widehat{\frac{\partial y(\rho)}{\partial \rho}}(t) = \begin{bmatrix} \hat{y}'(\rho(1))(t) & \hat{y}'(\rho(2))(t) & \dots & \hat{y}'(\rho(n_\rho))(t) \end{bmatrix} \in \mathbb{R}^{n_o \times N\rho}. \tag{22}$$

Then $E\left\{\widehat{\frac{\partial y(\rho)}{\partial \rho}}(t)\right\} = \frac{\partial y(\rho)}{\partial \rho}(t)$ and consequently,

$$E\{\hat{g}(\rho)\} = g(\rho). \tag{23}$$

Proof. For the entries of (20) it holds that $E\{a^{\alpha\beta}a^{\gamma\delta}\} = 1$ if $\alpha = \gamma$, $\beta = \delta$ and $E\{a^{\alpha\beta}a^{\gamma\delta}\} = 0$ otherwise. Therefore, (20) is equal to $\tilde{y}'(\rho(x)) + \eta$, with

$$\tilde{y}'(\rho(x)) = \begin{bmatrix} \sum_{k=1}^{n_i}\sum_{l=1}^{n_o} C'_{kl}(SP)_{1k}e_l \\ \vdots \\ \sum_{k=1}^{n_i}\sum_{l=1}^{n_o} C'_{kl}(SP)_{n_o k}e_l \end{bmatrix}, \tag{24}$$

and η containing all the terms for which $\alpha \neq \gamma$ or $\beta \neq \delta$. Since $E\{\eta\} = 0$, and since the SISO elements C'_{kl} and $(SP)_{1k}$ commute, it holds that

$$E\{\hat{y}'(\rho(x))\} = \tilde{y}'(\rho(x)) = y'(\rho(x)). \tag{25}$$

From (25) and (22) it follows that $E\left\{\widehat{\frac{\partial y(\rho)}{\partial \rho}}(t)\right\} = \frac{\partial y(\rho)}{\partial \rho}(t)$ and consequently, it holds that $E\{\hat{g}(\rho)\} = g(\rho)$. □

The unbiased estimate $\hat{g}(\rho)$ in Theorem 1 is obtained from a single experiment on SP, illustrated in Fig. 3 and given by

$$SPAe = \begin{bmatrix} (SP)_{11} & \dots & (SP)_{1n_i} \\ \vdots & \ddots & \vdots \\ (SP)_{n_o 1} & \dots & (SP)_{n_o n_i} \end{bmatrix} A \begin{pmatrix} e_1 \\ \vdots \\ e_{n_o} \end{pmatrix} = \begin{bmatrix} \sum_{k=1}^{n_i}(SP)_{1k}\left(\sum_{l=1}^{n_o} a^{kl}e_l\right) \\ \vdots \\ \sum_{k=1}^{n_i}(SP)_{n_o k}\left(\sum_{l=1}^{n_o} a^{kl}e_l\right) \end{bmatrix}. \tag{26}$$

Experiment (26) gives the terms $\sum_{k=1}^{n_i}(SP)_{ik}\left(\sum_{l=1}^{n_o} a^{kl}e_l\right)$ for $i = 1, \dots, n_o$, which are the entries of (20) that allow for computation of (22) and finally $\hat{g}(\rho)$.

Remark 2. In practice, experiment (26) often contains noise and disturbances, described by the term v in Fig. 3 but omitted in the experiment expressions for brevity. Under certain assumptions on v, see Section 4, the estimate $\hat{y}(\rho(x))$ obtained through experiment (26), as well as the gradient estimate, remain unbiased.

4. Stochastic approximation IFT using unbiased gradient estimates

In the previous section, it is shown that unbiased estimates of the gradient of (2) can be obtained efficiently from a single experiment on the closed-loop system, reducing the required number of experiments significantly compared to the existing MIMO IFT approach. In this section, these estimates are used in a stochastic gradient descent parameter update, leading to a stochastic approximation iterative feedback tuning (SAIFT) algorithm for minimizing (2). First, the parameter updates are introduced and second, convergence conditions are derived, constituting the second contribution.

4.1. Parameter updates

In order to minimize (2), the controller parameters ρ are updated iteratively in the direction of the unbiased gradient estimate $g(\rho_j)$ at iteration j. Each iteration, $g(\rho_j)$ is determined according to Theorem 1 and experiment (26), using an iteration-varying matrix A_j that is constructed according to (19).

The gradient estimates $\hat{g}(\rho)$ are used in a stochastic gradient descent update, given by

$$\rho_{j+1} = \rho_j - \varepsilon_j \hat{g}(\rho_j). \tag{27}$$

Here, ε_j denotes the step size. The method, including the two experiments required at each iteration to determine $e_j(\rho_j)$ and $\hat{g}(\rho_j)$, is summarized in Algorithm 1.

Algorithm 1 Efficient MIMO SAIFT

1: **for** $j = 0 : n_{\text{iteration}} - 1$
2: Experiment: for controller $C(\rho_j)$ and reference r, measure $e_j = r - y_j(\rho_j)$.
3: Experiment: using controller $C(\rho_j)$, input $A_j e_j$, and no reference, measure $SPA_j e_j$ according to (26).
4: Compute all estimates $\hat{y}'(\rho(x))$ according to (20).
5: Compute $\hat{g}(\rho_j)$ according to (21) and (22).
6: Update $\rho_{j+1} = \rho_j - \varepsilon_j \hat{g}_j$ according to (27).
7: **end**

4.2. Convergence

Next, conditions for the convergence of the SAIFT algorithm (27) are developed. In the previous section, the presence of noise and disturbances in the system evaluations was omitted for brevity. In practice, there are disturbances during experiments, included in the term v in Fig. 3, for which the following is assumed.

Assumption 1. The disturbance signal v is a bounded discrete-time zero-mean stochastic process. The second-order statistics are the same for all experiments, and sequences from different experiments are mutually independent.

Note that when a disturbance signal v is present in the experiments, two different realizations of e_j should be used for computing respectively $SPA_j e_j$ and $\hat{g}(\rho_j)$ to avoid bias, thus introducing an additional experiment. Then, Assumption 1 ensures that the gradient estimates $\hat{g}$ remain unbiased when disturbances are taken into account. The gradient estimate $\hat{g}(\rho_j)$ is rewritten as

$$\hat{g}(\rho_j) = g(\rho_j) + \omega_j. \tag{28}$$

Here, the disturbance term ω_j results from η_j in (20), which is propagated when (22) and $\hat{g}(\rho_j)$ are constructed. It contains both the unbiased stochastic terms resulting from the inclusion of A_j, and the propagation of the disturbance term v. Similar to η_j and v, for ω_j it holds that $E\{\omega_j\} = 0$ by Theorem 1 and Assumption 1. In addition, the choice of matrix A_j and Assumption 1 ensure that the sequence $\{w_j\}$ is square-integrable.

Using (28), the SAIFT algorithm is written as a Robbins–Monro algorithm:

$$\rho_{j+1} = \rho_j - \varepsilon_j(g(\rho_j) + \omega_j), \tag{29}$$

Consider the following assumptions, which are standard for these type of algorithms.

Assumption 2. The iterates ρ_j remain almost surely bounded.

Assumption 3. The step size ε_j is chosen such that

$$\sum_j^\infty \varepsilon_j = \infty, \qquad \sum_j^\infty \varepsilon_j^2 < \infty.$$

Assumptions 2 and 3 can be satisfied by choosing ε_j appropriately. However, in practice, satisfying Assumption 2 is not trivial. Even if the parameter iterate ρ_j is bounded, the resulting controller might lead to an unstable closed-loop system. This leads to an unbounded error $e(\rho_j)$ and consequently the gradient estimate and the next iterate ρ_{j+1} are unbounded. It is therefore essential that the parameter update leads to a stabilizing controller. This can be ensured by choosing ε_j small enough, but it is difficult to guarantee in practice, see also Section 6.1. Note that Assumption 2 also requires that the controller $C(\rho_j)$ is Lipschitz continuous, since the derivatives $C'(\rho_j(x))$ must remain bounded in order for ρ_j to remain bounded. In addition, the sequence $\{w_j\}$ is square integrable due to the choice of matrix A_j and Assumption 1.

The assumptions lead to the following theorem.

Theorem 2. *Under Assumptions 2 and 3, the sequence of iterates $\{\rho_j\}$ in (29) converges to a stationary point ρ^* for which $g(\rho) = 0$ almost surely.*

The disturbance term ω_j is a Martingale difference sequence since $E\{\omega_j\} = 0$ and it is square integrable. The proof of Theorem 2 follows from this property and the almost sure convergence of a Robbins–Monro algorithm under Assumption 2 and 3, see, e.g., Borkar (2008, Chapter 2).

Remark 3. Note that Theorem 2 is similar to the convergence theorem (Hjalmarsson & Kan Hjalmarsson, 1999, Theorem 1), which considers only the disturbance terms that are due to noisy system evaluations, and in which boundedness of the iterates is ensured by requiring that the closed-loop system remains stable. Again, this stability must be ensured by the user through a suitable choice of step size.

5. Comparison to MIMO IFT and non-full controllers

In this section, stochastic approximation IFT as developed in the previous two sections is compared to the existing experiment-intensive method for IFT for MIMO systems. In addition, the special case of MIMO controllers in which not all controller blocks are used, is considered for both SAIFT and IFT.

5.1. Experiment-intensive MIMO iterative feedback tuning

In the existing approach to MIMO IFT (Hjalmarsson & Birkeland, 1998), an unbiased estimate of the gradient of cost function (2) is generated through $n_i \times n_o$ noisy experiments on the $n_i \times n_o$ system. Here, the stochastic nature of the estimate results directly from the disturbances during the experiments, and for deterministic experiments this method leads to exact, deterministic gradients.

To illustrate how the term $\frac{\partial y(\rho)}{\partial \rho}(t)$ can be obtained through $n_i \times n_o$ experiments, consider again the derivatives $y'(\rho(x))$ in (11). Constructing this term requires only the signals $(SP)_{mk}(\rho)e_l(\rho)$ for $m = 1, \dots, n_o$, $k = 1, \dots, n_i$, $l = 1, \dots, n_o$. In MIMO IFT, these signals are obtained through $n_i \times n_o$ experiments, where in each experiment the measured error e_l from one of the output directions is injected between the controller and the plant in one of the n_i input directions k. This is illustrated in Fig. 4. With the $n_i \times n_o$ signals $(SP)_{mk}(\rho)e_l(\rho)$, all derivatives $y'(\rho(x))$ can be computed, leading to $\frac{\partial y(\rho)}{\partial \rho}(t)$ and finally the gradient $g(\rho)$.

An overview of the $n_i \times n_o + 1$ experiments needed for each iteration to determine $e_j(\rho_j)$ and $\hat{g}(\rho_j)$ in MIMO iterative feedback tuning is given in Algorithm 2.

Algorithm 2 Experiment-intensive MIMO IFT

for $j = 0 : n_{\text{iteration}} - 1$
  Experiment: for controller $C(\rho_j)$ and reference r, measure $e_j = r - y_j(\rho_j)$.
  for $l = 1 : n_o$
    for $k = 1 : n_i$
      Experiment: using controller $C(\rho_j)$, input $\begin{bmatrix} 0^{1\times(k-1)} & e_l(\rho_j)\mathsf{T} & 0^{1\times(n_i-k)} \end{bmatrix}\mathsf{T}$, and no reference, measure $y = (SP)_{mk}(\rho)e_l(\rho)$ for $m = 1, \dots, n_o$.
    end
  end
  Compute all derivatives $\hat{y}'(\rho(x))$ according to (11).
  Compute $\hat{g}(\rho_j)$ according to (4) and (7).
  Update $\rho_{j+1} = \rho_j - \varepsilon_j \hat{g}_j$ according to (27).
end

It is also possible to measure each derivative in a separate experiment by injecting $C'(\rho(x))e$ at the position of u, i.e., between the controller and the plant, in an experiment with $r = 0$. Obtaining the complete expression $\frac{\partial y(\rho)}{\partial \rho}(t)$ this way requires n_ρ experiments for n_ρ parameters, and since typically $n_\rho > n_i \times n_o$, this may require even more experiments. It follows that overall, this existing approach to MIMO IFT is experimentally inefficient for large MIMO systems, as is illustrated in the simulations and experimental results in the next sections.

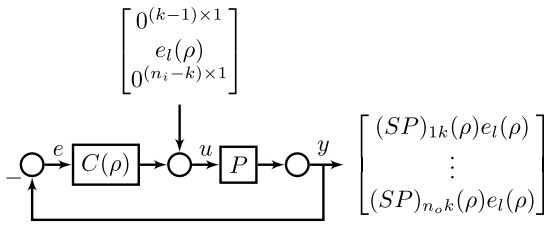

Fig. 4. In each of the $n_i \times n_o$ experiments required for MIMO iterative feedback tuning, the measured error e_l, $l = 1, \dots, n_o$, from one of the output directions is injected between the controller and the plant in one of the n_i input directions k, $k = 1, \dots, n_i$, resulting in n_o signals $(SP)_{mk}(\rho)e_l(\rho)$, $m = 1, \dots, n_o$. The noise term is omitted for brevity.

5.2. Non-full MIMO controllers

In cases where not all controller blocks are used, such as diagonal controllers, both MIMO IFT and SAIFT can be implemented more efficiently. In case of MIMO IFT, each controller block that is not used reduces the required number of experiments with one (Hjalmarsson & Kan Hjalmarsson, 1999). This is easily illustrated for the 2×2 example in Section 3.2. In the case that, for example, $C_{12} = 0$, the derivative $y'(\rho(x))$ in (13) reduces to

$$y'(\rho(x)) = \begin{bmatrix} (SP)_{11}C'_{11}e_1 + (SP)_{12}(C'_{21}e_1 + C'_{22}e_2) \\ (SP)_{21}C'_{11}e_1 + (SP)_{22}(C'_{21}e_1 + C'_{22}e_2) \end{bmatrix}, \tag{30}$$

since in this case $C'_{12} = 0$ also. As a result, the experiment with input $\begin{bmatrix} e_2^\mathsf{T} & 0 \end{bmatrix}$ is not necessary. If $C_{21} = 0$ also, then the experiment with input $\begin{bmatrix} 0 & e_1^\mathsf{T} \end{bmatrix}$ can be omitted also and only two experiments per iteration are needed for the diagonal controller. This extends directly to larger MIMO systems. In (11), each controller block C_{kl} that is zero removes all terms with $(SP)_{mk}e_l$ from the equation, and the experiment with input $\begin{bmatrix} 0^{1\times(k-1)} & e_l(\rho_j)^\mathsf{T} & 0^{1\times(n_i-k)} \end{bmatrix}^\mathsf{T}$ can be omitted.

In case of SAIFT, a similar step can be taken to reduce the variance in the single experiment needed for each iteration. In particular, it is possible to set $a_{kl} = 0$ if C_{kl} is zero. This element of matrix A corresponds to the terms $(SP)_{mk}e_l$ in (11), and taking $a_{kl} = 0$ ensures that the signal e_l is not injected in input k of the system. While this does not reduce the number of experiments needed in SAIFT, it does reduce the variance of the stochastic gradient estimate, which is likely to improve the efficiency of the method in terms of the number of iterations needed to converge.

Remark 4. It is also possible to reduce the variance of the gradient estimate for full MIMO controllers at the cost of additional experiments, by averaging the gradient estimates obtained using several realizations of the random matrix A_j. However, this is in general not expected to lead to improved efficiency in terms of the number of experiments needed to converge.

6. Implementation aspects

The application of IFT involves certain implementation aspects that are elaborated upon in this section. First, some approaches to ensure stability of the controller and boundedness of the iterates are suggested. Second, scaling of the gradient experiments is introduced and third, some methods for robust optimization are presented.

6.1. Choosing step sizes and ensuring stability

The convergence result in Theorem 1 requires that Assumption 2 is met, i.e., that the iterates remain bounded. To satisfy this assumption, the parameter update (27) must be chosen such that it results in a stabilizing controller $C(\rho_{j+1})$. This is essential for both SAIFT and standard MIMO IFT. In practice, it is necessary to assess the stability of the closed-loop system with $C(\rho_{j+1})$ before the controller is implemented, and if necessary the step size ε_j in (27) should be adapted until the parameter update results in a stabilizing controller. There are several approaches to assessing the stability of the system, some of which are listed below.

- A non-parametric model such as a frequency-response measurement can be used directly to assess stability, for example using the generalized Nyquist theorem for MIMO systems.
- A non-parametric model may be used to determine the generalized stability margin, and choose the step size such that the Vinnicombe distance (Vinnicombe, 1993) between a stabilizing controller and the controller update remains below this value, see also Kammer et al. (1998).
- In order to ensure robust stability, frequency-domain constraints such as developed in Heertjes et al. (2016) for SISO systems can be added to the optimization problem.
- An approximate parametric model of the system, combined with appropriate bounds to ensure robustness, can be used to assess stability.

These approaches all require at least a non-parametric model of the system, such as a frequency-response measurement, which are often relatively inexpensive, fast and accurate to obtain.

6.2. Scaling of experiments

The SAIFT approach in Algorithm 1 requires a dedicated experiment in which the measured error signal of the previous iteration, pre-multiplied with a random matrix A_j, is injected between the controller and the plant as illustrated in Fig. 3. In this type of experiment, it may be necessary to scale the input signal $A_j e_j$. While it is assumed that the system is linear, in practice most mechanical systems are subject to nonlinear effects such as static friction and actuator limits. A suitable scaling of the gradient experiment ensures that the system remains within the linear domain during the experiment and can be implemented using a scaling factor α by taking

$$S(\rho)PA_je_j = \frac{1}{\alpha_j}S(\rho)P\alpha_jA_je_j. \tag{31}$$

The scaling factor α_j is chosen separately for each iteration, because the magnitude of $A_j e_j$ depends strongly on A_j. Note that a similar scaling may be necessary for each of the $n_i \times n_o$ gradient experiments in standard MIMO IFT.

6.3. Methods for robust optimization

The cost function considered in IFT is typically non-convex, such that only local optimality may be achieved. In previous examples from literature, see, e.g., Hjalmarsson (2002), it has been observed that when the actual closed-loop response of the system is very different from the desired response, updating the controller in a direction of decreasing cost may lead to unexpected and undesired controller performance. Hjalmarsson (2002) suggests two approaches to avoid this problem, that can be directly applied to SAIFT. First, it is possible to choose the initial desired response as something that is relatively similar to the system response in a reference-model setting. In the setting without reference models that is considered here, this is comparable to choosing the initial reference such that the tracking error is limited. The performance requirements can then be increased successively in each iteration. Second, it is possible to include a time-varying weighting in the cost function (2) to reduce the weight in certain challenging parts of the reference.

A third approach that is particularly suitable to mechatronic systems is the use of feedforward control to reduce the initial error. Similar to the strategy of increasing the performance requirements iteratively, the feedforward contribution can be reduced iteratively to avoid too large

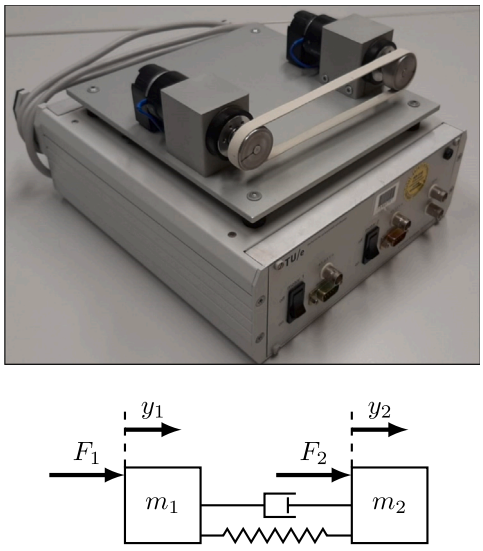

Fig. 5. Photo (top) and schematic representation (bottom) of the two-mass–spring–damper system with inputs F_1 and F_2 [V] and outputs y_1 and y_2 [rad].

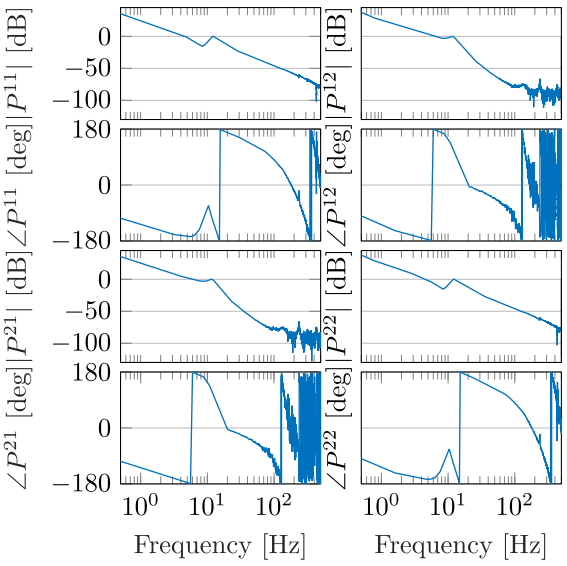

Fig. 6. Measured frequency response function of the system P. Note that this model information is not used in the IFT algorithms.

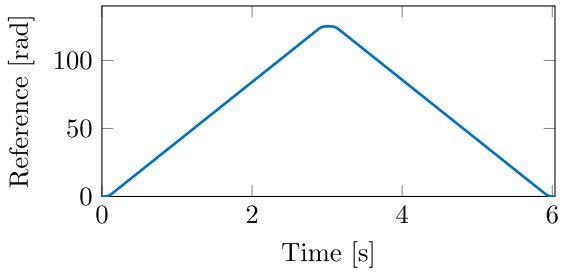

Fig. 7. The reference $r_1 = r_2$ is identical for both axes.

deviations between reference and system response. For mechatronic systems, suitable feedforward components are mass feedforward and compensation of viscous and static friction, implemented using the reference acceleration, velocity and sign of the velocity, see, e.g., Bolder, Oomen, Koekebakker, and Steinbuch (2014).

7. Application: experiments on a mechatronic system

In this section, the stochastic approximation IFT method developed in the previous sections is applied to a mechatronic system and compared to the existing experimentally-expensive IFT method, constituting the third contribution. First, the system is introduced and second, experimental results are presented.

7.1. Experimental setup

The experimental setup consists of two rotating masses that are connected by an elastic band that acts as a spring and a damper, as shown in Fig. 5. Both masses are actuated with inputs $\begin{bmatrix} F_1 & F_2 \end{bmatrix}^\mathsf{T}$, and the system output consists of the positions of both masses $\begin{bmatrix} y_1 & y_2 \end{bmatrix}^\mathsf{T}$. The system is sampled at 1 kHz such that the sampling time is $T_s = 0.001$ s. The dynamics of the 2×2 system P are shown in the measured frequency response function in Fig. 6, which illustrates that there is strong interaction between the two axis of the MIMO system. The system can be decoupled in a rigid-body and a flexible mode, resulting in a decoupled system P_{dec}, given by

$$P_{\text{dec}} = \begin{bmatrix} \frac{1}{2} & \frac{1}{2} \\ \frac{1}{2} & -\frac{1}{2} \end{bmatrix} \begin{bmatrix} P_{11} & P_{12} \\ P_{21} & P_{22} \end{bmatrix} \begin{bmatrix} 1 & 1 \\ 1 & -1 \end{bmatrix}. \tag{32}$$

First, a full MIMO controller that uses all controller channels is designed for the original plant P. Second, a decentralized controller is designed for the decoupled system P_{dec}. In this case, only two controller channels are used, leading to more efficient IFT implementations.

7.2. Experimental results: full MIMO controller

SAIFT and experimentally-intensive IFT are used to optimize a full MIMO controller for the original system P. All experiments use the same reference $r_1 = r_2$, shown in Fig. 7. The controller is constructed as a combination of a diagonal controller with two decoupling matrices, the parameters of which are free. The first element of the diagonal controller contains a proportional term, an integrator, a lead/lag filter and a lowpass filter. The second element consists of a proportional term and a lead/lag filter. This leads to a discrete-time controller of the form

$$C_{\text{full}}(\rho, z) = \tag{33}$$
$$\begin{bmatrix} \rho(9) & \rho(10) \\ \rho(11) & \rho(12) \end{bmatrix} \begin{bmatrix} C_{11}(\rho, z) & 0 \\ 0 & C_{22}(\rho, z) \end{bmatrix} \begin{bmatrix} \rho(13) & \rho(14) \\ \rho(15) & \rho(16) \end{bmatrix},$$
$$C_{11}(\rho, z) = \frac{T_s \rho(1) \left(\frac{2z-2}{2T_s \rho(3) \pi (z+1)} + 1 \right) \left(2\pi \rho(2) + \frac{z-1}{T_s} \right)}{\left(\frac{2z-2}{2T_s \rho(4) \pi (z+1)} + 1 \right) \left(\frac{2z-2}{2T_s \rho(5) \pi (z+1)} + 1 \right) (z-1)},$$
$$C_{22}(\rho, z) = \frac{T_s \rho(6) \left(\frac{2z-2}{2T_s \rho(7) \pi (z+1)} + 1 \right)}{\left(\frac{2z-2}{2T_s \rho(8) \pi (z+1)} + 1 \right)}.$$

The initial parameters are listed in Table 1, and the frequency response function of the initial controller is shown in Fig. 10. Since this full MIMO controller uses all controller channels, experimentally-intensive IFT requires four experiments to obtain a gradient estimate. In contrast, SAIFT requires only a single experiment with a full iteration-varying A-matrix of the form

$$A_j = \begin{bmatrix} a_j^{11} & a_j^{12} \\ a_j^{21} & a_j^{22} \end{bmatrix}, \tag{34}$$

The experimental results for both SAIFT and experiment-intensive IFT are shown in Figs. 8 and 9, using constant step sizes of respectively $\varepsilon = 0.1$ in Fig. 8 and $\varepsilon = 0.01$ in Fig. 9. The results demonstrate that SAIFT requires far fewer experiments to obtain the same cost compared to the experimentally-intensive method, while the number of iterations is approximately equal. In this case, the difference in accuracy between

Table 1
Controller parameters at iteration 0 and 50 for a full MIMO controller and a decentralized controller, both using SAIFT with $\varepsilon = 0.1$.

	ρ_0 MIMO	ρ_{50} MIMO	ρ_0 dec.	ρ_{50} dec.
$\rho_j(1)$	0.169	0.433	0.169	0.398
$\rho_j(2)$	$\frac{5}{3}$	1.685	$\frac{5}{3}$	1.663
$\rho_j(3)$	$\frac{5}{3}$	1.638	$\frac{5}{3}$	1.643
$\rho_j(4)$	15	15.00	15	15.00
$\rho_j(5)$	30	30.00	30	30.00
$\rho_j(6)$	4.640	4.620	4.640	4.627
$\rho_j(7)$	10	10.00	10	10.00
$\rho_j(8)$	90	90.00	90	90.00
$\rho_j(9)$	1	1.035	–	–
$\rho_j(10)$	1	1.041	–	–
$\rho_j(11)$	1	0.889	–	–
$\rho_j(12)$	−1	−1.015	–	–
$\rho_j(13)$	$\frac{1}{2}$	0.570	–	–
$\rho_j(14)$	$\frac{1}{2}$	0.313	–	–
$\rho_j(15)$	$\frac{1}{2}$	0.575	–	–
$\rho_j(16)$	$-\frac{1}{2}$	−0.514	–	–

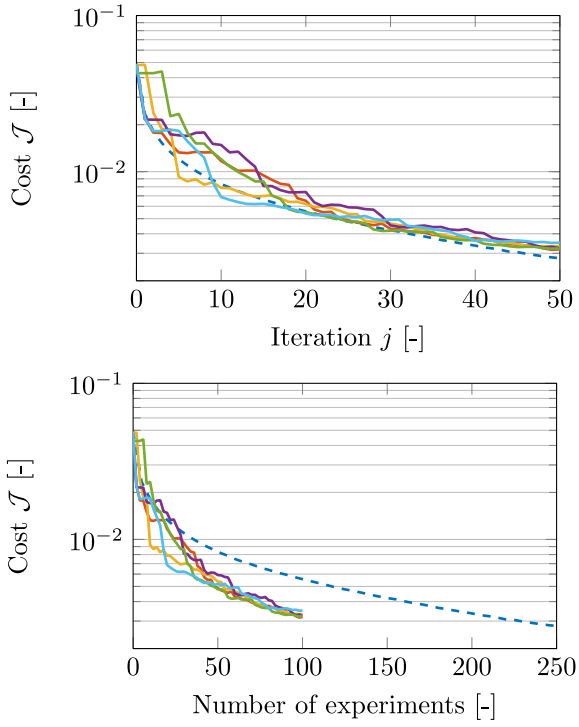

Fig. 8. Experimental results for a full MIMO controller using $\varepsilon = 0.1$. Five different SAIFT runs (—, —, —, —, —) require the same number of iterations to achieve a similar cost compared to experiment-intensive IFT (- -) (top), but SAIFT requires far fewer experiments (bottom).

the deterministic gradients and the gradient estimates does not influence the number of iterations required to converge. Comparison of the results for different step sizes shows that reducing the step size for SAIFT leads to a smoother convergence curve, but it also reduces the convergence speed.

The parameters and frequency response for the final controller for an SAIFT experiment with $\varepsilon = 0.1$ are shown in respectively Table 1 and Fig. 10. In addition, Fig. 11 depicts the change in the MIMO sensitivity function $S = (I + PC)^{-1}$ between iteration 0 and 50, and Fig. 12 shows the reduction in error. Interestingly, Fig. 10 seems to suggest that the main changes in the controller consist of an increased gain at frequencies below 1 Hz, yet Fig. 11 shows a reduction in sensitivity

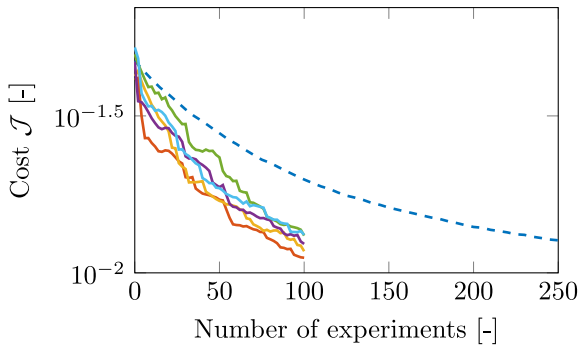

Fig. 9. Experimental results for a full MIMO controller using $\varepsilon = 0.01$. Five different SAIFT runs (—, —, —, —, —) each require far fewer experiments to achieve a similar cost compared to experiment-intensive MIMO IFT (- -).

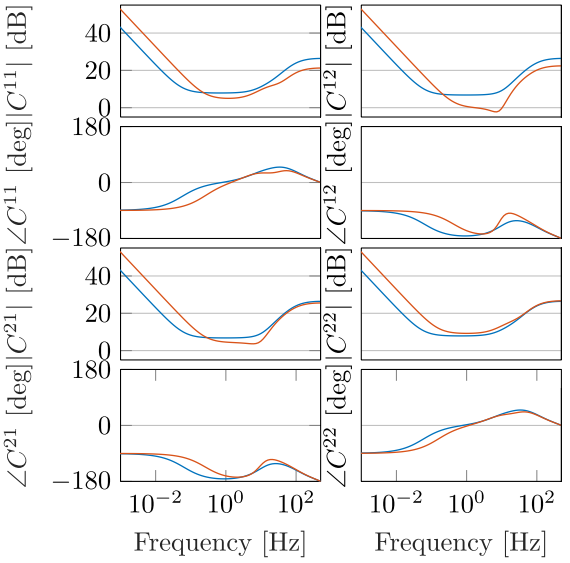

Fig. 10. Initial feedback controller C at iteration 0 (—) and final controller (—) at iteration 50 using SAIFT with $\varepsilon = 0.1$.

magnitude around 7 Hz instead, corresponding to the dominant frequency of the error in the constant-velocity part of the reference, cf. Fig. 12 in which this error component is indeed reduced. Fig. 11 also shows that in this case, the initial controller based on loop tuning was too conservative, and that the performance can be increased significantly when models are omitted and consequently, robustness margins such as $\sup_{\omega\in[0,2\pi)} \bar{\sigma}(S(e^{i\omega}))$ do not have to be taken into account. In addition, the differences between the changes in C and S illustrate that even for relatively simple MIMO systems, manual controller design is non-trivial, motivating the use of data-driven controller design.

7.3. Experimental results: decentralized controller

Next, SAIFT and experimentally-intensive IFT are used to design a decentralized controller for the decoupled MIMO system P_{dec}. The output and reference for the decoupled system are based on those for the original system and are given by

$$y_{\text{dec}} = \begin{bmatrix} \frac{1}{2} & \frac{1}{2} \\ \frac{1}{2} & -\frac{1}{2} \end{bmatrix} \begin{bmatrix} y_1 \\ y_2 \end{bmatrix}, \; r_{\text{dec}} = \begin{bmatrix} \frac{1}{2} & \frac{1}{2} \\ \frac{1}{2} & -\frac{1}{2} \end{bmatrix} \begin{bmatrix} r_1 \\ r_2 \end{bmatrix} = \begin{bmatrix} r_1 \\ 0 \end{bmatrix},$$

since $r_1 = r_2$. In these experiments, the cost function $\mathcal{J}_{\text{dec}}(\rho)$ to be minimized follows from replacing r and y in (2) by r_{dec} and y_{dec}, respectively.

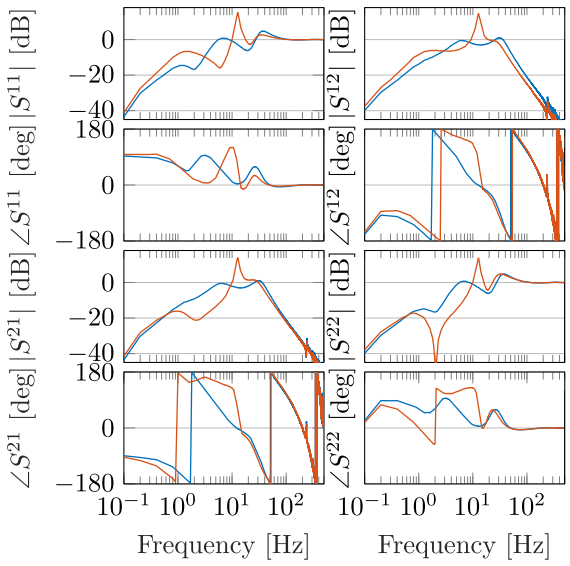

Fig. 11. Initial sensitivity function S at iteration 0 (—) and final sensitivity function (—) at iteration 50 using SAIFT with $\varepsilon = 0.1$.

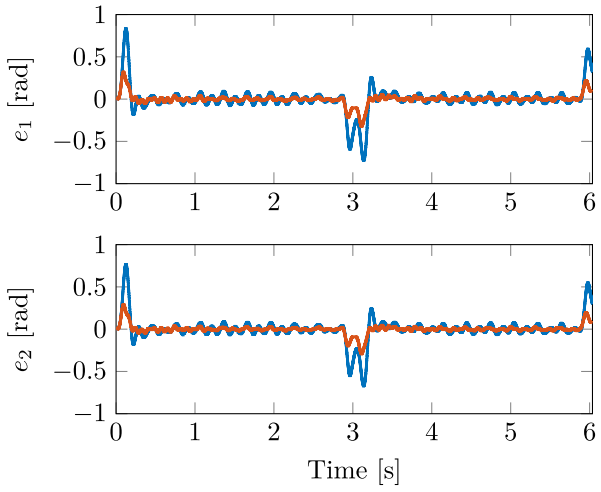

Fig. 12. Errors at iteration 0 (—) and 50 (—) while tuning a full MIMO controller using SAIFT with $\varepsilon = 0.1$.

The first element of the diagonal controller contains a proportional term, an integrator, a lead/lag filter and a lowpass filter. The second element consists of a proportional term and a lead/lag filter. The discrete-time transfer function of the controller is given by

$$C_{\text{diag}}(\rho, z) = \begin{bmatrix} C_{11}(\rho, z) & 0 \\ 0 & C_{22}(\rho, z) \end{bmatrix}, \text{ with} \tag{35}$$

$$C_{11}(\rho, z) = \frac{T_s\,\rho(1)\left(\frac{2z-2}{2T_s\,\rho(3)\,\pi\,(z+1)}+1\right)\left(2\,\pi\,\rho(2)+\frac{z-1}{T_s}\right)}{\left(\frac{2z-2}{2T_s\,\rho(4)\,\pi\,(z+1)}+1\right)\left(\frac{2z-2}{2T_s\,\rho(5)\,\pi\,(z+1)}+1\right)(z-1)},$$

$$C_{22}(\rho, z) = \frac{T_s\,\rho(6)\left(\frac{2z-2}{2T_s\,\rho(7)\,\pi\,(z+1)}+1\right)}{\left(\frac{2z-2}{2T_s\,\rho(8)\,\pi\,(z+1)}+1\right)}.$$

The initial parameters, as well as the parameters for iteration 50, are given in Table 1. Since C_{diag} is a diagonal controller with only two controller blocks, SAIFT can be implemented with a partial iteration-varying A-matrix of the form

$$A_j = \begin{bmatrix} a_j^{11} & 0 \\ 0 & a_j^{22} \end{bmatrix}, \tag{36}$$

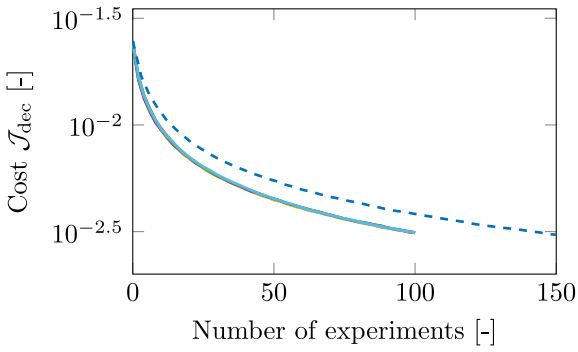

Fig. 13. Experimental results for a diagonal MIMO controller using $\varepsilon = 0.1$. Five different SAIFT runs (—, —, —, —, —) each require fewer experiments to achieve a similar cost compared to experiment-intensive MIMO IFT (- -).

as explained in Section 5.2. In this case, experimentally-intensive IFT requires two experiments to obtain a gradient estimate, whereas SAIFT requires only a single experiment. The step size is chosen as $\varepsilon = 0.1$. The experimental results are shown in Fig. 13 and demonstrate that SAIFT reduces the required number of experiments significantly. In addition, using only a partial A-matrix reduces the variance in the gradient estimates and leads to much smoother convergence, especially for this decoupled system for which the error of the flexible mode is close to zero.

8. Conclusion

The introduction of randomization in MIMO IFT reduces the number of experiments per iteration significantly, thus enabling broader applications of this model-free feedback tuning approach. A stochastic approximation IFT algorithm is presented that obtains unbiased gradient estimates from a single randomized experiment. The gradient estimates are used in a stochastic gradient descent parameter update, and the convergence is analyzed. Experimental implementation on a mechatronic system demonstrates that SAIFT requires far fewer experiments to reach the same cost compared to the existing, experiment-intensive MIMO IFT approach.

CRediT authorship contribution statement

Leontine Aarnoudse: Writing – review & editing, Writing – original draft, Methodology, Formal analysis, Conceptualization. **Peter den Toom:** Visualization, Validation, Software. **Tom Oomen:** Writing – review & editing, Supervision, Investigation, Funding acquisition, Conceptualization.

Declaration of competing interest

The authors declare that they have no known competing financial interests or personal relationships that could have appeared to influence the work reported in this paper.

References

Aarnoudse, L., & Oomen, T. (2021). Model-free learning for massive MIMO systems: Stochastic approximation adjoint iterative learning control. *IEEE Control Systems Letters*, *5*(6), 1946–1951. http://dx.doi.org/10.1109/LCSYS.2020.3046169.

Aarnoudse, L., & Oomen, T. (2023). Efficient MIMO iterative feedback tuning via randomization. In *Conf. decis. control* (pp. 4512–4517). http://dx.doi.org/10.1109/CDC49753.2023.10383883.

Baciu, A., & Lazar, C. (2023). Iterative feedback tuning of model-free intelligent PID controllers. *Actuators*, *12*(2), 56. http://dx.doi.org/10.3390/act12020056.

Bolder, J., Kleinendorst, S., & Oomen, T. (2018). Data-driven multivariable ILC: Enhanced performance by eliminating l and q filters. *International Journal of Robust and Nonlinear Control*, *28*(12), 3728–3751. http://dx.doi.org/10.1002/rnc.3611.

Bolder, J., Oomen, T., Koekebakker, S., & Steinbuch, M. (2014). Using iterative learning control with basis functions to compensate medium deformation in a wide-format inkjet printer. *Mechatronics*, *24*(8), 944–953. http://dx.doi.org/10.1016/j.mechatronics.2014.07.003.

Borkar, V. S. (2008). *Stochastic approximation: A dynamical systems viewpoint*. Cambridge University Press, http://dx.doi.org/10.1007/978-93-86279-38-5.

Campi, M. C., Lecchini, A., & Savaresi, S. M. (2002). Virtual reference feedback tuning: a direct method for the design of feedback controllers. *Automatica*, *38*, 1337–1346. http://dx.doi.org/10.1016/j.automatica.2005.02.008, URL www.elsevier.com/locate/automatica.

Codrons, B., De Bruyne, F., De Wan, M., & Gevers, M. (1998). Iterative feedback tuning of a nonlinear controller for an inverted pendulum with a flexible transmission. *IEEE Conference on Control Technology and Applications*, *2*(September), 1281–1285. http://dx.doi.org/10.1109/cca.1998.721667, URL http://ieeexplore.ieee.org/document/721667/.

Formentin, S., Bisoffi, A., & Oomen, T. (2015). Asymptotically exact direct data-driven multivariable controller tuning. *Vol. 48*, In *17th IFAC symp. syst. identif.* (pp. 1349–1354). Beijing, China: http://dx.doi.org/10.1016/j.ifacol.2015.12.319.

Formentin, S., & Savaresi, S. M. (2011). Noniterative data-driven design of multivariable controllers. *Proc. IEEE Conf. Decis. Control*, 5106–5111. http://dx.doi.org/10.1109/CDC.2011.6160388.

Gerencsér, L., Vágó, Z., & Hjalmarsson, H. (2002). Randomized iterative feedback tuning. *Vol. 35*, In *15th trienn. IFAC world congr.* (pp. 361–366). Barcelona, Spain: http://dx.doi.org/10.3182/20020721-6-ES-1901.01046.

Hamamoto, K., Fukuda, T., & Sugie, T. (2003). Iterative feedback tuning of controllers for a two-mass-spring system with friction. *Control Engineering Practice*, *11*(9), 1061–1068. http://dx.doi.org/10.1016/S0967-0661(02)00229-0.

Heertjes, M. F., Van Der Velden, B., & Oomen, T. (2016). Constrained iterative feedback tuning for robust control of a wafer stage system. *IEEE Transactions on Control Systems Technology*, *24*(1), 56–66. http://dx.doi.org/10.1109/TCST.2015.2418311.

Hildebrand, R., Lecchini, A., Solari, G., & Gevers, M. (2004). Prefiltering in iterative feedback tuning: Optimization of the prefilter for accuracy. *IEEE Transactions on Automatic Control*, *49*(10), 1801–1805. http://dx.doi.org/10.1109/TAC.2004.835598.

Hjalmarsson, H. (2002). Iterative feedback tuning - an overview. *International Journal of Adaptive Control and Signal Processing*, *16*(5), 373–395. http://dx.doi.org/10.1002/acs.714.

Hjalmarsson, H. (2005). From experiment design to closed-loop control. *Automatica*, *41*(3), 393–438. http://dx.doi.org/10.1016/j.automatica.2004.11.021.

Hjalmarsson, H. H., & Birkeland, T. (1998). Iterative feedback tuning of linear time-invariant MIMO systems. In *Proc. IEEE conf. decis. control* (pp. 3893–3898). http://dx.doi.org/10.1109/cdc.1998.761837.

Hjalmarsson, H., Gevers, M., Gunnarsson, S., & Lequin, O. (1998). Iterative feedback tuning: Theory and applications. *IEEE Control System*, *18*(4), 26–41. http://dx.doi.org/10.1109/37.710876, URL https://ieeexplore.ieee.org/document/710876/.

Hjalmarsson, H., & Kan Hjalmarsson, H. S. (1999). Efficient tuning of linear multivariable controllers using iterative feedback tuning. *International Journal of Adaptive Control and Signal Processing*, *13*, 553–572. http://dx.doi.org/10.1002/(SICI)1099-1115(199911)13:7<553::AID-ACS572>3.0.CO;2-B.

Huusom, J. K., Hjalmarsson, H., Poulsen, N. K., & Jørgensen, S. B. (2011). A design algorithm using external perturbation to improve iterative feedback tuning convergence. *Automatica*, *47*(12), 2665–2670. http://dx.doi.org/10.1016/j.automatica.2011.05.029.

Kammer, L. C., Bitmead, R. R., & Bartlett, P. L. (1998). Direct iterative tuning via spectral analysis. *Automatica*, *36*(9), 2874–2879. http://dx.doi.org/10.1016/S0005-1098(00)00040-6, URL https://linkinghub.elsevier.com/retrieve/pii/S0005109800000406.

Kissling, S., Blanc, P., Myszkorowski, P., & Vaclavik, I. (2009). Application of iterative feedback tuning (IFT) to speed and position control of a servo drive. *Control Engineering Practice*, *17*(7), 834–840. http://dx.doi.org/10.1016/j.conengprac.2009.02.005.

Mišković, L., Karimi, A., Bonvin, D., & Gevers, M. (2007). Correlation-based tuning of decoupling multivariable controllers. *Automatica*, *43*(9), 1481–1494. http://dx.doi.org/10.1016/j.automatica.2007.02.006.

Oomen, T., Van Der Maas, R., Rojas, C. R., & Hjalmarsson, H. H. (2014). Iterative data-driven H-infinity norm estimation of multivariable systems with application to robust active vibration isolation. *IEEE Transactions on Control Systems Technology*, *22*(6), 2247–2260. http://dx.doi.org/10.1109/TCST.2014.2303047.

Robbins, H., & Monro, S. (1951). A stochastic approximation method. *The Annals of Mathematical Statistics*, *22*(3), 400–407.

Roman, R.-C. C., Precup, R.-E. E., Hedrea, E.-L. L., Preitl, S., Zamfirache, I. A., Bojan-Dragos, C.-A. A., et al. (2022). Iterative feedback tuning algorithm for tower crane systems. *Procedia Computer Science*, *199*, 157–165. http://dx.doi.org/10.1016/j.procs.2022.01.020.

Sanfelice Bazanella, A., Campestrini, L., & Eckhard, D. (2012). *Data-Driven Controller Design*. Springer, http://dx.doi.org/10.1007/978-94-007-2300-9.

Solari, G., & Gevers, M. (2004). Unbiased estimation of the hessian for iterative feedback tuning (ift). In *43rd IEEE conf. decis. contol* (pp. 1759–1760). Nassau, Bahamas: http://dx.doi.org/10.1109/CDC.2004.1430299.

Spall, J. C. J. (1988). Stochastic approximation algorithm for large-dimensional systems in the kiefer-wolfowitz setting. In *Proc. IEEE conf. decis. control* (pp. 1544–1548). IEEE, http://dx.doi.org/10.1109/cdc.1988.194588, URL http://ieeexplore.ieee.org/document/194588/.

Tesch, D. A., Eckhard, D., & Guarienti, W. C. (2016). Pitch and roll control of a quadcopter using cascade iterative feedback tuning. *IFAC-PapersOnLine*, *49*(30), 30–35. http://dx.doi.org/10.1016/j.ifacol.2016.11.118.

Vinnicombe, G. (1993). Frequency domain uncertainty and the graph topology. *IEEE Transactions on Automatic Control*, *38*(9), 1371–1383. http://dx.doi.org/10.1109/9.237648.

Xie, Y., Jin, J., Tang, X., Ye, B., & Tao, J. (2019). Robust cascade path-tracking control of networked industrial robot using constrained iterative feedback tuning. *IEEE Access*, *7*, 8470–8482. http://dx.doi.org/10.1109/ACCESS.2018.2889702.